

Extraordinary Temperature Dependent Second Harmonic Generation in Atomically Thin Layers of Transition-Metal Dichalcogenides

Ahmed Raza Khan, Boqing Liu, Linglong Zhang, Yi Zhu, Xin He, Lijun Zhang, Tiejun Lü,* and Yuerui Lu*

Atomically thin transition metal dichalcogenides (TMDs) are important semi-conducting materials because of their interesting layer dependent properties. Recently, optical second harmonic generation (SHG) is used to probe layer number, lattice orientation, phase variation, and strain vector in ultrathin TMDs. Here, it is demonstrated that SHG response of ultrathin TMDs is highly sensitive to temperature modulation. Furthermore, temperature dependent SHG is found to show opposite trends for single layer and few odd layers (3L, 5L, 7L, etc.) of TMDs. A remarkable temperature dependent SHG enhancement (25.8%) is found in single layer molybdenum diselenide (MoSe_2) using 900 nm laser excitation whereas few odd layers show significant temperature dependent SHG quenching which is found to be -55.2% , -31.02% , and -18.4% in case of 3L, 5L, and 7L of MoSe_2 . Temperature dependent SHG investigation with other TMDs, like MoS_2 , WS_2 , and WSe_2 , shows the similar trend which reveals an important structural characteristic for TMDs. Second order nonlinear susceptibility calculations considering weak van der Waal forces during thermal expansion in ultrathin TMDs show good agreement with the experimental findings. The results show SHG as a powerful and sensitive approach to investigate thermal variation in ultrathin TMDs.

1. Introduction

Currently, there is an increased research interest in 2D layered materials^[1–10] because of their exciting layer dependent properties. For instance, transition metal dichalcogenides (TMDs) are semiconducting layered materials which exhibit promising layer dependent optical and electronic properties.^[11–15] For instance, one layer (1L) molybdenum diselenide (MoSe_2) is a direct bandgap semiconductor material with enhanced photoluminescence (PL) properties. On the other hand, 2L MoSe_2 is an indirect bandgap semiconductor with low PL emission.^[16,17] The remarkable layer dependent properties of TMDs suggest their potential to be used in nanoscale optical and electronic device fabrication.^[18–27]

Temperature is found to alter optoelectronic properties such as bandgap modulation,^[17] variation in phonon modes,^[28–31] and tuning in carrier mobility^[32–36] in

nano materials. Therefore, it is important to investigate the layer dependent thermal variation in 2D TMDs in order to better control and optimize the performance of electronic devices. Recently, optical second-harmonic generation (SHG) have shown high sensitivity to lattice symmetry, therefore, SHG effect is used to probe lattice symmetry,^[37] lattice variation,^[31] strain direction and intensity,^[38–40] and mechanical pressure^[41] in 2D layered materials. Thermal variation causes significant structural variation in 2D TMD which makes SHG a potentially useful and powerful tool to investigate thermal changes in ultrathin TMDs. In this work, we show SHG as a highly sensitive tool to investigate the thermal variation in ultrathin TMDs. Moreover, an opposite SHG trend is observed for single layer and few odd layers (3L, 5L, 7L, etc.) of TMDs. In this regard, a remarkable SHG enhancement (25.8%) in single layer MoSe_2 is found with rise in temperature. On the other hand, few odd layers show considerable temperature dependent SHG quenching for 3L (-55.2%), 5L (-31.02%), and 7L (-18.4%) of MoSe_2 . Other TMD materials, like, MoS_2 , WS_2 , and WSe_2 show the similar trend which reveals an important structural characteristic for TMDs. Nonlinear susceptibility calculations considering thermal expansion behavior for single layer and

A. R. Khan, B. Liu, Dr. L. Zhang, Y. Zhu, Prof. Y. Lu
Research School of Electrical Energy and Materials Engineering
College of Engineering and Computer Science
Australian National University
Canberra, ACT 2601, Australia
E-mail: yuerui.lu@anu.edu.au

A. R. Khan
Department of Industrial and Manufacturing Engineering
University of Engineering and Technology (Rachna College)
Lahore 54700, Pakistan

X. He, L. Zhang
Key Laboratory of Automobile Materials of MOE and College
of Materials Science and Engineering
Jilin University
Changchun 130012, China

Dr. T. Lü
Department of Physics
and Institute of Theoretical Physics and Astrophysics
Xiamen University
Xiamen 361005, China
E-mail: mailoliver@126.com

 The ORCID identification number(s) for the author(s) of this article can be found under <https://doi.org/10.1002/adom.202000441>.

DOI: 10.1002/adom.202000441

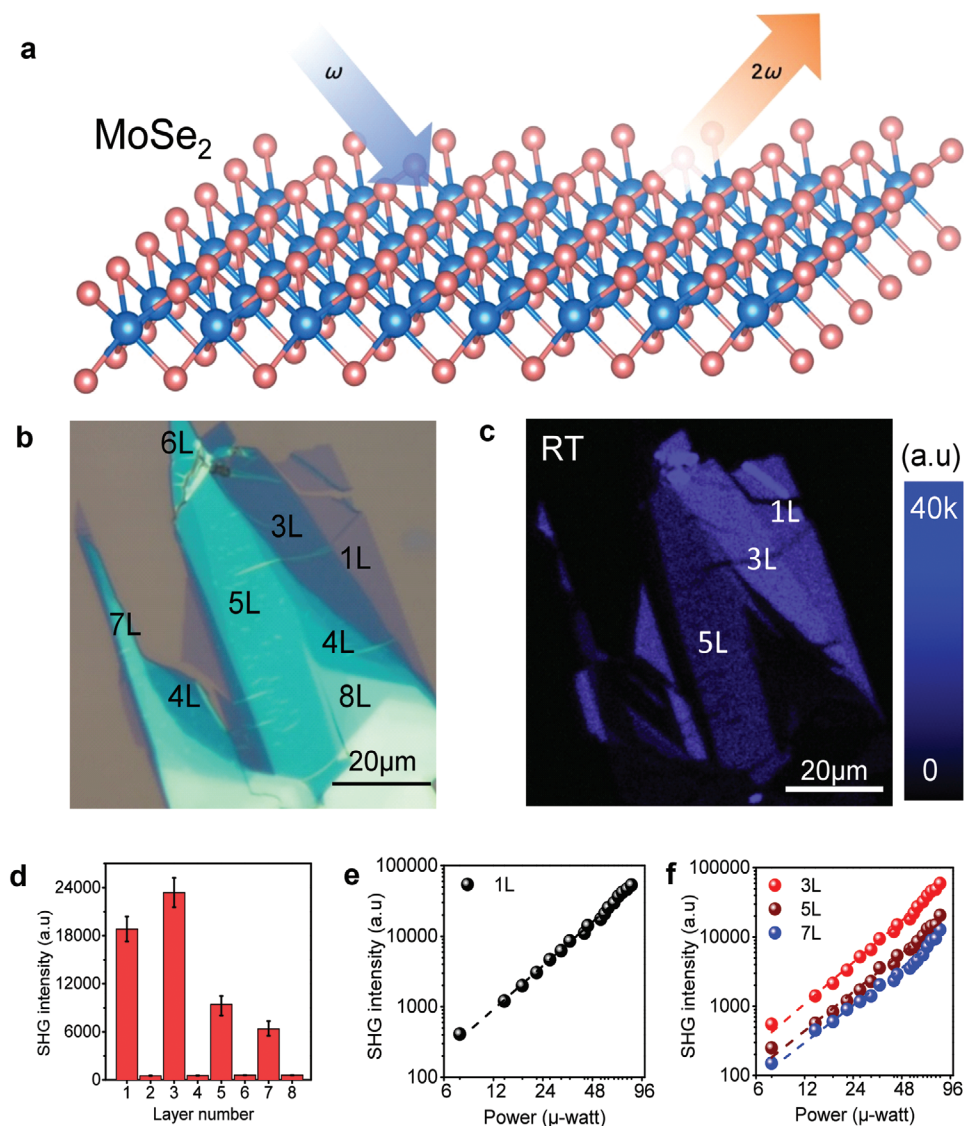


Figure 1. Layer dependent second harmonic generation in MoSe₂. a) Schematic illustration of the SHG process, two photons of the same frequency ω merge into a single photon with double frequency 2ω . b) Optical microscopic image of 1–8L MoSe₂ for second harmonic generation (SHG) mapping. c) SHG image of (b) showing the layer dependent SHG response (laser excitation: 900 nm). d) Column chart showing layer dependent SHG response of 1–8L MoSe₂. Histogram shows the SHG intensity response, with variation in measurements indicated by the error bars. Power dependent SHG of e) 1L and f) 3L, 5L, and 7L. (Note: All the SHG measurements are taken at 900 nm laser excitation.)

few layers TMD explains the layer dependent temperature dependent SHG behavior, which shows good agreement with the experimental findings. Our results show SHG as a powerful and sensitive probe to monitor thermal variation in layered TMDs.

2. Results and Discussions

In our experiment, few-layered MoSe₂ flakes are mechanically exfoliated onto a Si/SiO₂ (275 nm) chip substrate using a scotch tape, following the prescription of Ref. [42–44]. MoSe₂ layers are identified by their color contrast on an optical microscope as shown in **Figure 1b**. Variable colors contrast indicate height variation. Phase-shifting interferometry^[45–49] is used

to identify the layer number of ultrathin MoSe₂ as shown in Figure S1a,b, Supporting Information. Confocal light microscope (Zeiss 780) with 900 nm laser excitation is employed for second harmonic generation (SHG) (see methods section for more details). SHG mapping of 1–8L MoSe₂ at room temperature is done in order to check the layer dependent SHG response as shown in **Figure 1c**. Even layers of MoSe₂ belong to the centrosymmetric D_{3d} space group, whereas odd layer number belongs to the non-centrosymmetric D_{3h} space group, therefore, we get SHG signal from odd layer number, such as, 1L, 3L, 5L, and 7L and we do not get SHG response from even layer number, such as, 2L, 4L, 6L, and 8L (**Figure 1d**), consistent with the previous studies^[37,38,50,51] which show SHG a sensitive probe to lattice symmetry. As SHG shows quadratic scaling behavior,^[52–55] therefore, power

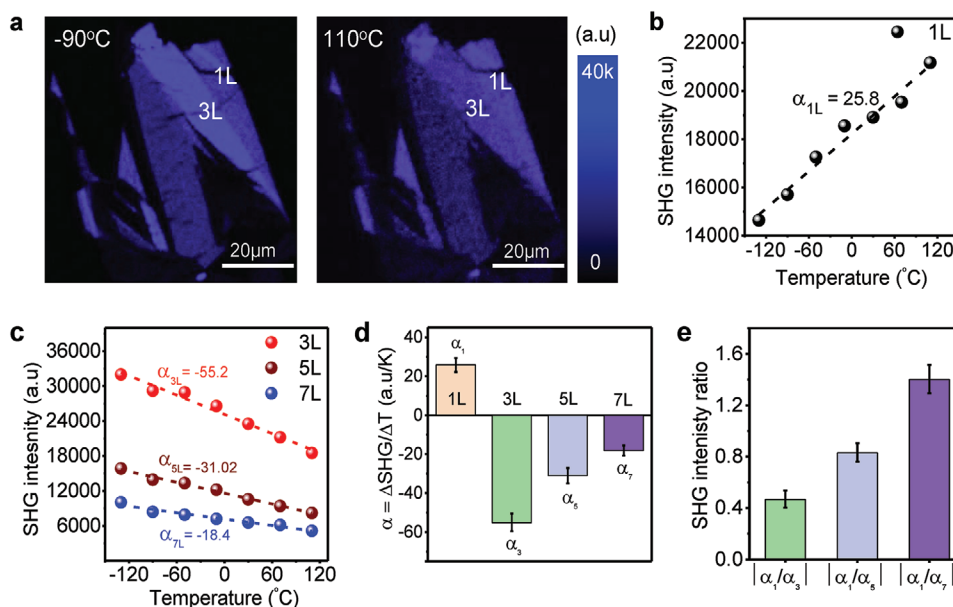


Figure 2. Temperature dependent SHG of layered MoSe₂. a) Second harmonic mapping of 1–8L MoSe₂ sample at –90 °C and 110 °C. Temperature dependent SHG response of b) 1L and c) 3L, 5L, and 7L, where dashed lines indicate the linear fits; α_1 , α_3 , α_5 , and α_7 indicate the slopes of the linear fit dashed lines for 1L, 3L, 5L, and 7L. d) Layer dependent temperature dependent SHG slope values (α_1 , α_3 , α_5 , and α_7). The variation in the measurements is indicated by the error bars. e) SHG slope ratios (α_1/α_3), (α_1/α_5), and (α_1/α_7) for MoSe₂. (All the SHG measurements are taken at 900 nm laser excitation.)

dependent SHG measurements are performed for all the odd layers (1L, 3L, 5L, and 7L) in order to confirm the existence of SH photons. The corresponding SHG signal responses for each odd layer were drawn with excitation power on a log scale^[56–58] as shown in Figure 1e,f. The obtained slope values ≈ 2.0 confirm the SHG.

In order to determine the temperature dependent SHG behavior, temperature controller equipped with liquid nitrogen and heating source is used to tune the temperature of the sample (for more details see Methods section). SHG intensity mappings are performed at variable temperature settings ranging from –130 °C to 110 °C for 1–8L MoSe₂ using 900 nm laser excitation as shown in Figure 2a–c. Even layers of MoSe₂ do not show SHG response at all scanned temperatures. Interestingly, single layer and few odd layers of MoSe₂ show opposite temperature dependent SHG behavior. SHG intensity of 1L MoSe₂ increases with the temperature whereas few odd layers of MoSe₂ such as, 3L, 5L, and 7L show the opposite trend. The measured temperature dependence of SHG fits linearly and α_1 , α_3 , α_5 , and α_7 represent the slopes of the linear fitted lines for 1L, 3L, 5L, and 7L. The measurements show $\alpha_1 = 25.8 \pm 3.5$ (brown), $\alpha_3 = -55.2 \pm 4.5$ (green), $\alpha_5 = -31.02 \pm 4$ (blue), and $\alpha_7 = -18.2 \pm 3$ (purple) for MoSe₂ as shown in Figure 2d (variation in values is indicated by the error bars). SHG slopes ratios α_1/α_3 (green), α_1/α_5 (blue), and α_1/α_7 (purple) are shown in Figure 2e which show the increasing trend of α_1/α_n as layer number “n” increases.

The temperature dependent SHG investigation indicates SHG is sensitive to thermal variation in MoSe₂. In order to find the temperature dependent SHG behavior with other layer dependent TMDs, we performed temperature dependent layer dependent SHG measurements for layer

dependent WSe₂, WS₂, and MoS₂ at the same laser excitation that is, 900 nm (Figure 3a–e). SHG mappings indicate that temperature dependent SHG for other TMDs shows the similar behavior like thermal investigation in MoSe₂. For instance, SHG response of 1L WSe₂ increases with the temperature whereas 3L WSe₂ show a decreasing SHG response (Figure 3a,b). Similarly, SHG intensity for higher few layers such as 5L, 7L decreases with the rise in temperature. Layer dependent WS₂ (Figure 3c,d) and MoS₂ (Figure 3e) show the similar trend. Here, we find the temperature dependent SHG slope values as under; $\alpha_1 = 63.12 \pm 7.00$, $\alpha_3 = -33.22 \pm 5.16$, and $\alpha_5 = -29.74 \pm 4.98$ for WS₂, $\alpha_1 = 18.29 \pm 2.91$, $\alpha_3 = -25.72 \pm 3.93$, $\alpha_5 = -21.51 \pm 4.07$, and $\alpha_7 = -14.02 \pm 3.28$ for WSe₂, and $\alpha_1 = 93.03 \pm 8.91$, $\alpha_3 = -57.99 \pm 6.84$, $\alpha_5 = -52.89 \pm 6.46$, and $\alpha_7 = -43.97 \pm 4.22$ for MoS₂ (Figure 3f). Temperature dependent SHG slope ratios (1L to 3L, 5L, and 7L) indicate $\alpha_1/\alpha_3 = 1.9 \pm 0.165$ and $\alpha_1/\alpha_5 = 2.18 \pm 0.18$ for WS₂, $\alpha_1/\alpha_3 = 0.71 \pm 0.068$, $\alpha_1/\alpha_5 = 0.85 \pm 0.075$, and $\alpha_1/\alpha_7 = 1.304 \pm 0.115$ for WSe₂, and $\alpha_1/\alpha_3 = 1.6 \pm 0.1$, $\alpha_1/\alpha_5 = 1.76 \pm 0.11$, and $\alpha_1/\alpha_7 = 2.11 \pm 0.16$ for MoS₂ as shown in Figure 3g which show similar temperature dependent SHG behavior for other TMDs. As temperature dependent SHG behavior for other TMDs is found similar and SHG response is sensitive to variation in lattice structure, SHG behavior indicates an important structural characteristic for TMDs. Therefore, we explore the thermal expansion behavior of TMDs to understand and explain the temperature dependent SHG in TMDs layers.

The optical field of the SHG is proportional to the non-linear optical susceptibility; therefore, the relation between SHG intensity and crystal lattice can be shown by calculating second order nonlinear susceptibility considering thermal expansion in layer dependent TMDs. Phase matching is an

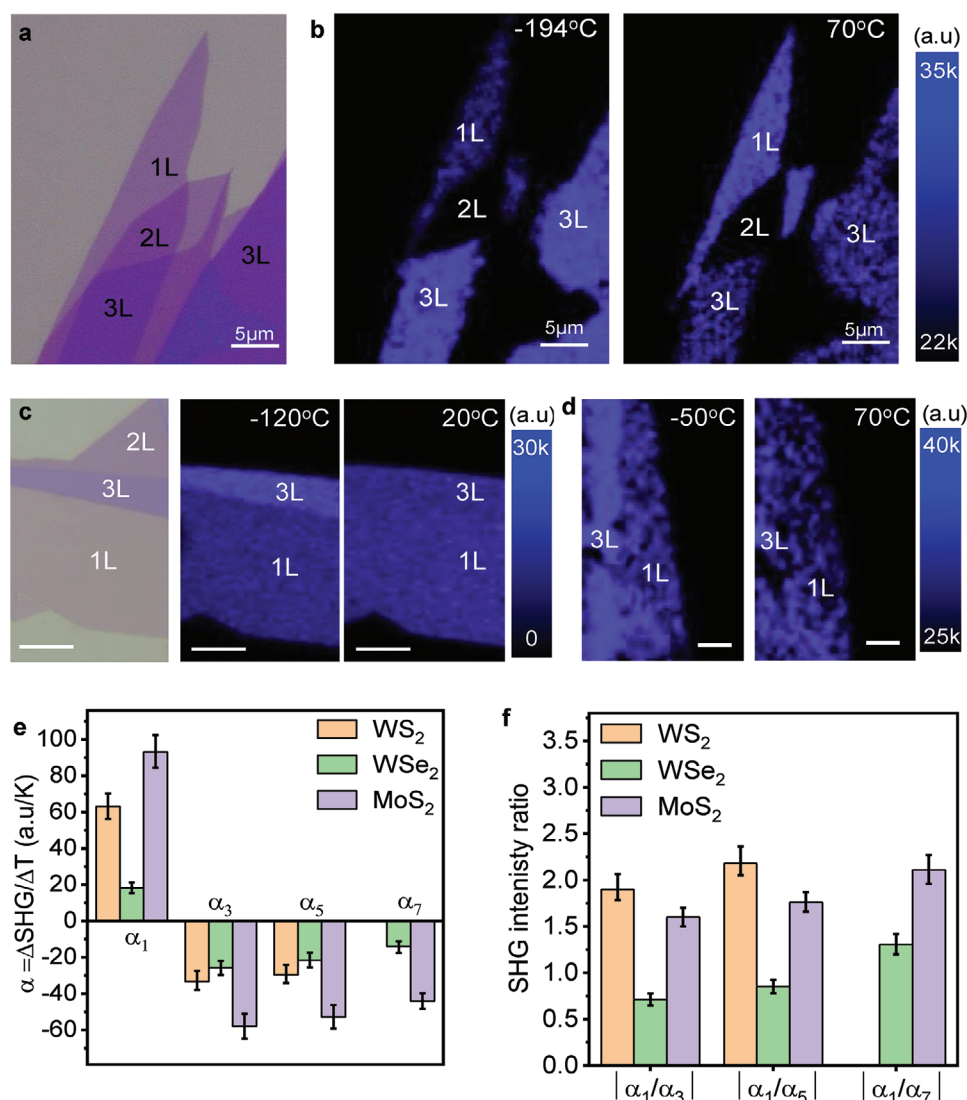


Figure 3. Temperature dependent SHG of other layered transition metal dichalcogenides (TMDs). a) Optical microscope image of 1–3L WSe₂ sample used for SHG mapping. b) Temperature dependent SHG mapping of WSe₂ at –194 °C and 70 °C. c) Optical microscope image of 1–3L WS₂ sample. d) Temperature dependent SHG mapping of WS₂ sample at –120 °C and 20 °C. e) Temperature dependent SHG mapping of the sample at –50 °C and 70 °C. (Note: All scale bars indicate 5 μm length, laser excitation = 900 nm) f) Layer dependent temperature dependent SHG slope values (α) for WS₂, WSe₂, and MoS₂. g) SHG slope ratios for WSe₂, WSe₂, and MoSe₂. A variation in measurements is indicated by the error bars.

important condition for SHG efficiency, therefore, conventional nonlinear materials have certain limitations for usage in future nonlinear photonic devices^[59–62] due to phase matching issues. Extraordinary SHG discovery in 2D TMDs including monolayer/multilayer MoS₂,^[37,63,64] MoSe₂,^[65] WS₂,^[56] and WSe₂,^[66] is interesting which is attributed to their perfect phase matching.^[59] Because 2D TMDs have a thickness far below the optical coherence length,^[51,59] thus eliminating the requirement for phase matching for ultrathin TMDs and hence, for their small thermal expansion ($\approx 10^{-5}$ – 10^{-6} K⁻¹).^[67,68] In this regard, we employ first-principles density functional theory (DFT)^[69] using simulation code Abinit to calculate the second order nonlinear susceptibility $I\chi(-2\omega, \omega, \omega)$.^[56] Exchange-correlation function within the local density approximation^[70] and a k -point sampling for the Brillouin zone integration are used. An energy cutoff

of 52Ry for the plane wave basis and a k -point sampling of $30 \times 30 \times 1$ is applied in the simulation. A vacuum layer thicker than 10 Å is added to avoid the mirror interaction. Dynamical stability of the crystal structures is confirmed by phonon dispersion from density functional perturbation theory calculations. We speculate that thermal expansion behavior in TMD layers might lead to the opposite SHG responses in 1L and few odd layers of TMDs. Few layers and bulk TMDs, with weak van der Waal forces (X-X) between vertically stacked layers, show higher thermal expansion than 1L TMDs in interlayer direction.^[71] Therefore, we consider van der Waal gap during thermal expansion behavior in few odd layers of TMDs. In 1L MoS₂, vertical lattice parameter is represented by “ d ” or (S–Mo–S) bond length and horizontal lattice parameter is represented by “ a ” 1L MoS₂ (TMD) as shown in Figure 4a. Lattice parameters

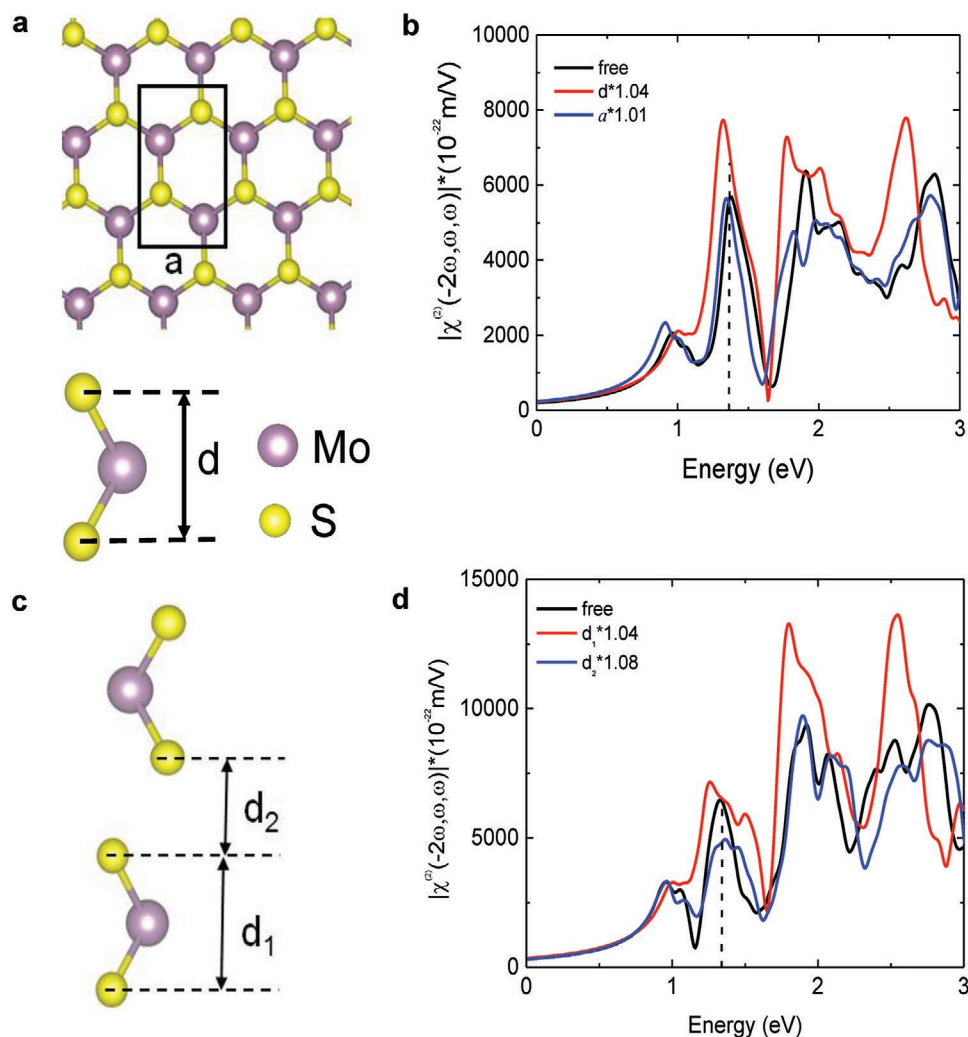


Figure 4. Temperature dependent nonlinear susceptibilities in 1L and 3L of TMDs. a) 1L MoS₂ (side view) showing intralayer attraction as represented by (S–M–S) bond length d (side view) and lattice constant a (top view). As temperature increases, d increases greater than a . b) Second-order nonlinear susceptibility calculation for 1L with 4% increase in d shows enhancement in nonlinear susceptibility response as compared to free 1L. c) Few layer MoS₂ showing intralayer attraction as represented by (S–M–S) bond length d_1 and van der Waal gap d_2 between two layers. As temperature increases, d_2 increases greater than d_1 . d) Second-order nonlinear susceptibility calculation for few layers with 8% increase in d_2 shows quenching in nonlinear susceptibility as compared to free few layers.

increase with the rise in temperature. Thermal expansion of the vertical lattice parameter (d) is reported to be greater than thermal expansion of horizontal lattice parameter (a).^[72] Therefore, we have calculated the second order nonlinear susceptibility $I\chi(-2\omega, \omega, \omega)$ (mV) of 1L MoS₂ for three cases; (i) free 1L MoS₂, (ii) 4% increase in d , and (iii) 1% increase in a . DFT calculations show that nonlinear susceptibility ($I\chi$) decreases as horizontal lattice parameter (a) increases whereas nonlinear susceptibility ($I\chi$) shows an enhancement with increase in d (Figure 4b) which explains the SHG enhancement with temperature in 1L TMDs. Few layers in TMDs are under the influence of interlayer attraction forces from other layers which are of van der Waal's type.^[73–76] Therefore, in comparison with 1L, few layers and bulk TMDs are reported with comparatively higher out-of-plane expansion coefficient as compared to in-plane expansion coefficient.^[71,72] This directional dependence thermal

expansion behavior can lead to variable lattice symmetries for 1L and few odd layers of TMDs showing us the opposite SHG behavior for 1L and few layers TMDs. This interlayer attraction due to S–S bond length is represented by van der Waal's gap d_2 as shown in Figure 4c. On the other hand, d_1 indicates the vertical intralayer attraction due to S–M–S bond length. Van der Waal forces of attraction are considered weak forces of attraction as compared to intralayer forces of attraction, therefore, d_2 is expected to increase considerably greater than d_1 with temperature increase. We have calculated the second order nonlinear susceptibility $I\chi(-2\omega, \omega, \omega)$ (mV) for few layers of MoS₂ for three cases; (i) free few layer MoS₂, (ii) 4% increase in d_1 , and (iii) 8% increase in d_2 . nonlinear susceptibility calculations show that $I\chi(-2\omega, \omega, \omega)$ decreases as d_2 increases for few layers MoS₂ as shown in Figure 4d. The considerable increase of d_2 with temperature shows SHG quenching. Thus, the calculated

results of 1L and few layers for temperature dependent second order nonlinear susceptibility show good agreement with our experimental findings.

3. Conclusion

In conclusion, we have shown that SHG response is highly sensitive to temperature modulation in 2D TMD. Temperature variation in ultrathin TMDs is found to tune SHG response which has variable trend for single layer and few odd layers (3L, 5L, 7L, etc.) of TMDs. 1L MoSe₂ shows remarkable SHG enhancement (25.8%) in single layer MoSe₂ with temperature increase. On the other hand, few odd layers show considerable SHG quenching which is found to be -55.2%, -31.02%, and -18.4% in case of 3L, 5L, and 7L of MoSe₂. Other TMDs materials, like MoS₂, WS₂ and WSe₂ show the similar trend which reveals an important structural characteristic for TMDs. Second order nonlinear susceptibility calculations considering weak van der Waal forces during thermal expansion in ultrathin TMDs show good agreement with the experimental findings. Our results would pave the way to enable novel applications of TMDs in nonlinear optical devices.

4. Experimental Section

Sample Fabrication: The SHG measurements were performed on Zeiss 780 Confocal Microscopy with repetition rate \approx 80 MHz and 150 fs pulse width (Ti:sapphire) tunable pulse. SHG measurements were taken at 900 nm laser excitation. The reflected SH signal was collected by the same objective, separated by a beam splitter and filtered by suitable optical filters to block the reflected fundamental radiation. The SH character of the detected radiation was verified by its wavelength and quadratic power dependence on the pump intensity. For temperature dependent measurements, the sample was placed into a Linkam THMS 600 chamber. A temperature controller equipped with a heating source (thermos-couples) and cooling source (liquid nitrogen) was used to control the temperature of the sample.

Supporting Information

Supporting Information is available from the Wiley Online Library or from the author.

Acknowledgements

A.R.K., B.L. and L.Z. contributed equally to this work. This work was supported in part by the Australian National University, Australia and Faculty Development Program funding under University of Engineering and Technology (Rachna College Campus) Lahore, Pakistan. The authors would like to acknowledge the financial support from ANU scholarship of Australia National University and Faculty Development Program (FDP) under University of Engineering and Technology (RCET campus), Pakistan. The authors acknowledge the Center of Advanced Microscopy (CAM) in Australian National University for their facility support.

Conflict of Interest

The authors declare no conflict of interest.

Keywords

layer dependence, optical second harmonic generation, temperature dependence, transition metal dichalcogenides

Received: March 13, 2020

Revised: April 23, 2020

Published online:

- [1] G. P. Neupane, W. Ma, T. Yildirim, Y. Tang, L. Zhang, Y. Lu, *Nano-mater. Sci.* **2019**, *1*, 246.
- [2] J. Pei, J. Yang, T. Yildirim, H. Zhang, Y. Lu, *Adv. Mater.* **2019**, *31*, 1706945.
- [3] K. Cho, J. Yang, Y. Lu, *J. Mater. Res.* **2017**, *32*, 2839.
- [4] R. Xu, J. Yang, Y. Zhu, H. Yan, J. Pei, Y. W. Myint, S. Zhang, Y. Lu, *Nanoscale* **2016**, *8*, 129.
- [5] T. Vogl, R. Lecomwasam, B. C. Buchler, Y. Lu, P. K. Lam, *ACS Photonics* **2019**, *6*, 1955.
- [6] T. Vogl, M. W. Doherty, B. C. Buchler, Y. Lu, P. K. Lam, *Nanoscale* **2019**, *11*, 14362.
- [7] T. Vogl, G. Campbell, B. C. Buchler, Y. Lu, P. K. Lam, *ACS Photonics* **2018**, *5*, 2305.
- [8] T. Vogl, Y. Lu, P. Koy Lam, *J. Phys. D: Appl. Phys.* **2017**, *50*, 295101.
- [9] T. Ahmed, S. Kuriakose, S. Abbas, M. J. S. Spencer, M. A. Rahman, M. Tahir, Y. Lu, P. Sonar, V. Bansal, M. Bhaskaran, S. Sriram, S. Walia, *Adv. Funct. Mater.* **2019**, *29*, 1901991.
- [10] J. Lu, J. Yang, A. Carvalho, H. Liu, Y. Lu, C. H. Sow, *Acc. Chem. Res.* **2016**, *49*, 1806.
- [11] C. Cong, J. Shang, Y. Wang, T. Yu, *Adv. Opt. Mater.* **2018**, *6*, 1700767.
- [12] K. F. Mak, J. Shan, *Nat. Photonics* **2016**, *10*, 216.
- [13] X. Duan, C. Wang, A. Pan, R. Yu, X. Duan, *Chem. Soc. Rev.* **2015**, *44*, 8859.
- [14] A. R. Khan, T. Lu, W. Ma, Y. Lu, Y. Liu, *Adv. Electron. Mater.* **2020**, *6*, 1901381.
- [15] K. F. Mak, J. Shan, *Nat. Photonics* **2016**, *10*, 216.
- [16] Y. Zhang, T.-R. Chang, B. Zhou, Y.-T. Cui, H. Yan, Z. Liu, F. Schmitt, J. Lee, R. Moore, Y. Chen, H. Lin, H.-T. Jeng, S.-K. Mo, Z. Hussain, A. Bansil, Z.-X. Shen, *Nat. Nanotechnol.* **2014**, *9*, 111.
- [17] B. K. Choi, M. Kim, K.-H. Jung, J. Kim, K.-S. Yu, Y. J. Chang, *Nanoscale Res. Lett.* **2017**, *12*, 492.
- [18] Q. H. Wang, K. Kalantar-Zadeh, A. Kis, J. N. Coleman, M. S. Strano, *Nat. Nanotechnol.* **2012**, *7*, 699.
- [19] W. Hsu, Z. Zhao, L. Li, C. Chen, M. Chiu, P. Chang, *ACS Nano* **2014**, *8*, 2951.
- [20] Y. Zhu, J. Yang, S. Zhang, S. Mokhtar, J. Pei, X. Wang, Y. Lu, *Nanotechnology* **2016**, *27*, 135706.
- [21] L. Britnell, R. M. Ribeiro, A. Eckmann, R. Jalil, B. D. Belle, A. Mishchenko, Y. J. Kim, R. V. Gorbachev, T. Georgiou, S. V. Morozov, A. N. Grigorenko, A. K. Geim, C. Casiraghi, A. H. C. Neto, K. S. Novoselov, *Science* **2013**, *340*, 1311.
- [22] J. Pei, J. Yang, X. Wang, F. Wang, S. Mokkapatil, T. Lü, J.-C. Zheng, Q. Qin, D. Neshev, H. H. Tan, C. Jagadish, Y. Lu, *ACS Nano* **2017**, *11*, 7468.
- [23] H. Chen, V. Corbolioiu, A. S. Solntsev, D.-Y. Choi, M. A. Vincenti, D. de Gellia, C. de Angelis, Y. Lu, D. N. Neshev, *Light: Sci. Appl.* **2017**, *6*, e17060.
- [24] N. K. Balla, M. O'Brien, N. McEvoy, G. S. Duesberg, H. Rigneault, S. Brasselet, D. McCloskey, *ACS Photonics* **2018**, *5*, 1235.
- [25] C. Ruppert, O. B. Aslan, T. F. Heinz, *Nano Lett.* **2014**, *14*, 6231.
- [26] S. Ahmed, J. Yi, *Nano-Micro Lett.* **2017**, *9*, 50.
- [27] E. Blundo, M. Felici, T. Yildirim, G. Pettinari, D. Tedeschi, A. Miriametro, B. Liu, W. Ma, Y. Lu, A. Polimeni, *Phys. Rev. Res.* **2020**, *2*, 012024.

- [28] M. Thripuranthaka, R. V. Kashid, C. Sekhar Rout, D. J. Late, *Appl. Phys. Lett.* **2014**, *104*, 081911.
- [29] S. Sahoo, A. P. S. Gaur, M. Ahmadi, M. J.-F. Guinel, R. S. Katiyar, *J. Phys. Chem. C* **2013**, *117*, 9042.
- [30] S. Sinha, V. Sathe, S. K. Arora, *Solid State Commun.* **2019**, *298*, 113626.
- [31] A. Mobaraki, C. Sevik, H. Yapicioglu, D. Çakır, O. Gülseren, *Phys. Rev. B* **2019**, *100*, 035402.
- [32] T. M, D. J. Late, *ACS Appl. Mater. Interfaces* **2014**, *6*, 1158.
- [33] A. Sharma, A. Khan, Y. Zhu, R. Halbach, W. Ma, Y. Tang, B. Wang, Y. Lu, *Nano Lett.* **2019**, *19*, 7877.
- [34] I. Yang, Z. Li, J. Wong-Leung, Y. Zhu, Z. Li, N. Gagrani, L. Li, M. N. Lockrey, H. Nguyen, Y. Lu, H. H. Tan, C. Jagadish, L. Fu, *Nano Lett.* **2019**, *19*, 3821.
- [35] L. Zhang, H. Yan, X. Sun, M. Dong, T. Yildirim, B. Wang, B. Wen, G. P. Neupane, A. Sharma, Y. Zhu, J. Zhang, K. Liang, B. Liu, H. T. Nguyen, D. Macdonald, Y. Lu, *Nanoscale* **2019**, *11*, 418.
- [36] L. Zhang, A. Sharma, Y. Zhu, Y. Zhang, B. Wang, M. Dong, H. T. Nguyen, Z. Wang, B. Wen, Y. Cao, B. Liu, X. Sun, J. Yang, Z. Li, A. Kar, Y. Shi, D. Macdonald, Z. Yu, X. Wang, Y. Lu, *Adv. Mater.* **2018**, *30*, 1803986.
- [37] Y. Li, Y. Rao, K. F. Mak, Y. You, S. Wang, C. R. Dean, T. F. Heinz, *Nano Lett.* **2013**, *13*, 3329.
- [38] L. Mennel, M. M. Furchi, S. Wachter, M. Paur, D. K. Polyushkin, T. Mueller, *Nat. Commun.* **2018**, *9*, 516.
- [39] J. Liang, J. Zhang, Z. Li, H. Hong, J. Wang, Z. Zhang, X. Zhou, R. Qiao, J. Xu, P. Gao, Z. Liu, Z. Sun, S. Meng, K. Liu, D. Yu, *Nano Lett.* **2017**, *17*, 7539.
- [40] R. Khan, B. Liu, W. Ma, L. Zhang, A. Sharma, Y. Zhu, T. Lü, Y. Lu, arXiv:2002.03631, **2020**.
- [41] D. Tedeschi, E. Blundo, M. Felici, G. Pettinari, B. Liu, T. Yildirim, E. Petroni, C. Zhang, Y. Zhu, S. Sennato, Y. Lu, A. Polimeni, *Adv. Mater.* **2019**, *31*, 1903795.
- [42] S. A. Han, R. Bhatia, S.-W. Kim, *Nano Converg.* **2015**, *2*, 17.
- [43] X. Li, H. Zhu, *J. Mater.* **2015**, *1*, 33.
- [44] H. Li, J. Wu, Z. Yin, H. Zhang, *Acc. Chem. Res.* **2014**, *47*, 1067.
- [45] J. Pei, J. Yang, R. Xu, Y.-H. Zeng, Y. W. Myint, S. Zhang, J.-C. Zheng, Q. Qin, X. Wang, W. Jiang, Y. Lu, *Small* **2015**, *11*, 6384.
- [46] J. Yang, Z. Wang, F. Wang, R. Xu, J. Tao, S. Zhang, Q. Qin, B. Luther-Davies, C. Jagadish, Z. Yu, Y. Lu, *Light: Sci. Appl.* **2016**, *5*, e16046.
- [47] Y. Wang, C. Cong, W. Yang, J. Shang, N. Peimyoo, Y. Chen, J. Kang, J. Wang, W. Huang, T. Yu, *Nano Res.* **2015**, *8*, 2562.
- [48] J. Pei, X. Gai, J. Yang, X. Wang, Z. Yu, D.-Y. Choi, B. Luther-Davies, Y. Lu, *Nat. Commun.* **2016**, *7*, 10450.
- [49] Y. Zhu, Z. Li, L. Zhang, B. Wang, Z. Luo, J. Long, J. Yang, L. Fu, Y. Lu, *ACS Appl. Mater. Interfaces* **2018**, *10*, 43291.
- [50] W. Wu, L. Wang, Y. Li, F. Zhang, L. Lin, S. Niu, D. Chenet, X. Zhang, Y. Hao, T. F. Heinz, J. Hone, Z. L. Wang, *Nature* **2014**, *514*, 470.
- [51] H. Wang, X. Qian, *Nano Lett.* **2017**, *17*, 5027.
- [52] L. M. Malard, T. V. Alencar, A. P. M. Barboza, K. F. Mak, A. M. De Paula, *Phys. Rev. B* **2013**, *87*, 201401.
- [53] J. Xiao, Z. Ye, Y. Y. Wang, H. Zhu, Y. Y. Wang, X. Zhang, *Light: Sci. Appl.* **2015**, *4*, e366.
- [54] T. Jiang, H. Liu, D. Huang, S. Zhang, Y. Li, X. Gong, Y.-R. Shen, W.-T. Liu, S. Wu, *Nat. Nanotechnol.* **2014**, *9*, 825.
- [55] A. Säynätjoki, L. Karvonen, H. Rostami, A. Autere, S. Mehravar, A. Lombardo, R. A. Norwood, T. Hasan, N. Peyghambarian, H. Lipsanen, K. Kieu, A. C. Ferrari, M. Polini, Z. Sun, *Nat. Commun.* **2017**, *8*, 2005.
- [56] C. Janisch, Y. Wang, D. Ma, N. Mehta, A. L. Elías, N. Perea-López, M. Terrones, V. Crespi, Z. Liu, *Sci. Rep.* **2014**, *4*, 5530.
- [57] K. L. Seyler, J. R. Schaibley, P. Gong, P. Rivera, A. M. Jones, S. Wu, J. Yan, D. G. Mandrus, W. Yao, X. Xu, *Nat. Nanotechnol.* **2015**, *10*, 407.
- [58] N. Kumar, S. Najmaei, Q. Cui, F. Ceballos, P. M. Ajayan, J. Lou, H. Zhao, *Phys. Rev. B* **2013**, *87*, 161403.
- [59] M. Zhao, Z. Ye, R. Suzuki, Y. Ye, H. Y. Zhu, J. Xiao, Y. Wang, Y. Iwasa, X. Zhang, *Light: Sci. Appl.* **2016**, *5*, e16131.
- [60] A. Rose, D. R. Smith, *Opt. Mater. Express* **2011**, *1*, 1232.
- [61] A. Autere, H. Jussila, Y. Dai, Y. Wang, H. Lipsanen, Z. Sun, *Adv. Mater.* **2018**, *30*, 1705963.
- [62] A. J. Stentz, R. W. Boyd, in *Handbook of Photonics*, 2nd ed. (Ed.: M. C. Gupta), CRC Press, Boca Raton **1997**.
- [63] L. M. Malard, T. V. Alencar, A. P. M. Barboza, K. F. Mak, A. M. De Paula, *Phys. Rev. B* **2013**, *87*, 201401.
- [64] R. I. Woodward, R. T. Murray, C. F. Phelan, R. E. P. De Oliveira, T. H. Runcorn, E. J. R. Kelleher, S. Li, E. C. De Oliveira, G. J. M. Fechine, G. Eda, C. J. S. De Matos, *2D Mater.* **2017**, *4*, 011006.
- [65] C. T. Le, D. J. Clark, F. Ullah, V. Senthilkumar, J. I. Jang, Y. Sim, M. J. Seong, K. H. Chung, H. Park, Y. S. Kim, *Ann. Phys.* **2016**, *528*, 551.
- [66] H. G. Rosa, Y. W. Ho, I. Verzhbitskiy, M. J. F. L. Rodrigues, T. Taniguchi, K. Watanabe, G. Eda, V. M. Pereira, J. C. V. Gomes, *Sci. Rep.* **2018**, *8*, 10035.
- [67] X. Hu, P. Yasaei, J. Jokisaari, S. Ögüt, A. Salehi-Khojin, R. F. Klie, *Phys. Rev. Lett.* **2018**, *120*, 055902.
- [68] L. Zhang, Z. Lu, Y. Song, L. Zhao, B. Bhatia, K. R. Bagnall, E. N. Wang, *Nano Lett.* **2019**, *19*, 4745.
- [69] W. Kohn, L. J. Sham, *Phys. Rev.* **1965**, *140*, A1133.
- [70] B. Lee, L. W. Wang, C. D. Spataru, S. G. Louie, *Phys. Rev. B* **2007**, *76*, 245114.
- [71] C. K. Gan, Y. Y. F. Liu, *Phys. Rev. B* **2016**, *94*, 134303.
- [72] S. H. El-Mahalawy, B. L. Evans, *J. Appl. Crystallogr.* **1976**, *9*, 403.
- [73] Y. Aray, D. Vega, J. Rodriguez, A. B. Vidal, D. S. Coll, *J. Comput. Methods Sci. Eng.* **2009**, *9*, 257.
- [74] C. Li, B. Fan, W. Li, L. Wen, Y. Liu, T. Wang, K. Sheng, Y. Yin, *J. Korean Phys. Soc.* **2015**, *66*, 1789.
- [75] A. Ostadhosseini, A. Rahnamoun, Y. Wang, P. Zhao, S. Zhang, V. H. Crespi, A. C. T. Van Duin, *J. Phys. Chem. Lett.* **2017**, *8*, 631.
- [76] R. Addou, L. Colombo, R. M. Wallace, *ACS Appl. Mater. Interfaces* **2015**, *7*, 11921.